View metadata, citation and similar papers at core.ac.uk
brought to you by CORE
provided by Elsevier - Publisher Connector

Cellular Signalling 26 (2014) 1725–1734

Contents lists available at ScienceDirect

Cellular Signalling

journal homepage: www.elsevier.com/locate/cellsig

Reduced phosphorylation of Stat3 at Ser-727 mediated by casein kinase 2 — Protein phosphatase 2A enhances Stat3 Tyr-705 induced tumorigenic potential of glioma cells

Tapashi Mandal [a], Arijit Bhowmik [a], Anirban Chatterjee [a], Uttara Chatterjee [b], Sandip Chatterjee [b], Mrinal Kanti Ghosh [a,*]

[a] Division of Cancer Biology and Inflammatory Disorder, CSIR—Indian Institute of Chemical Biology, 4, Raja S. C. Mullick Road, Kolkata 700032, India
[b] Division of Pathology, Park Clinic, 4, Gorky Terrace, Kolkata 700017, India

ARTICLE INFO

Article history:
Received 7 January 2014
Received in revised form 4 April 2014
Accepted 4 April 2014
Available online 12 April 2014

Keywords:
pStat3^{S727}
pStat3^{Y705}
CK2
PP2A
Glioma

ABSTRACT

Signal transducer and activator of transcription 3 (Stat3) is a transcription factor that is involved in cell survival and proliferation and has been found to be persistently activated in most human cancers mainly through its phosphorylation at Tyr-705. However, the role and regulation of Stat3 Ser-727 phosphorylation in cancer cells have not been clearly evaluated. In our findings, correlation studies on the expression of CK2 and Stat3 Ser-727 phosphorylation levels in human glioma patient samples as well as rat orthotopic tumor model show a degree of negative correlation. Moreover, brain tumor cell lines were treated with various pharmacological inhibitors to inactivate the CK2 pathway. Here, increased Stat3 Ser-727 phosphorylation upon CK2 inhibition was observed. Overexpression of CK2 (α, α′ or β subunits) by transient transfection resulted in decreased Stat3 Ser-727 phosphorylation. Stat3 Tyr-705 residue was conversely phosphorylated in similar situations. Interestingly, we found PP2A, a protein phosphatase, to be a mediator in the negative regulation of Stat3 Ser-727 phosphorylation by CK2. In vitro assays prove that Ser-727 phosphorylation of Stat3 affects the transcriptional activity of its downstream targets like SOCS3, bcl-xl and Cyclin D1. Stable cell lines constitutively expressing Stat3 S727A mutant showed increased survival, proliferation and invasion which are characteristics of a cancer cell. Rat tumor models generated with the Stat3 S727A mutant cell line formed more aggressive tumors when compared to the Stat3 WT expressing stable cell line. Thus, in glioma, reduced Stat3 Ser-727 phosphorylation enhances tumorigenicity which may be regulated in part by CK2–PP2A pathway.

© 2014 The Authors. Published by Elsevier Inc. This is an open access article under the CC BY-NC-ND license (http://creativecommons.org/licenses/by-nc-nd/3.0/).

1. Introduction

Glioblastoma multiforme (GBM) is the most aggressive and malignant form of brain tumor in human with very short patient survival [1]. Amongst the many causal reasons of GBM, alterations and perturbations in the molecular signaling pathways play a major role. Several signaling pathways have been implicated in the progression of GBM including phosphoinositide-3-kinase (PI3K), Ras-MAPK and tyrosine kinase signaling pathways viz. EGFR and VEGFR [2].

Apart from these conventional pathways, kinases like CK2 are now emerging as crucial molecules for GBM progression [3]. CK2 is a ubiquitous and highly conserved serine/threonine kinase with two alpha (catalytic) and two beta (regulatory) subunits [4]. This protein has been involved in the regulation of cellular growth and proliferation, transformation, apoptosis and senescence [5,6]. Increased expression and activity of CK2 in several cancers mark it as an important target for specific therapies [6]. Elevated levels of this protein have also been reported in human GBM tumor specimens where inhibition of CK2 could sensitize these cells to tumor necrosis factor-α induced apoptosis [7]. A CK2 inhibitor has been reported to induce antitumor activity in mouse xenograft model of human glioblastoma [8] while apigenin, another CK2 inhibitor, was found to modulate DNA damage response of GBM cells though it could not radiosensitize them [9]. CK2 can also induce glioma cell invasion by mediating α-catenin phosphorylation

Abbreviations: Stat3, signal transducer and activator of transcription 3; CK2, casein kinase 2; PP2A, protein phosphatase 2A; pStat3^{S727}, phosphoStat3 Ser-727; pStat3^{Y705}, phosphoStat3 Tyr-705; GBM, glioblastoma multiforme; EV, empty vector; qRT-PCR, quantitative real time polymerase chain reaction; WCL, whole cell lysate; SDS-PAGE, Sodium Dodecyl Sulfate Polyacrylamide Gel Electrophoresis; IP, immunoprecipitation; FACS, fluorescence activated cell sorting; RT, room temperature; PBS, Phosphate Buffered Saline; PI, propidium iodide; CPCSEA, committee for the purpose of control and supervision on experiments on animals.

* Corresponding author at: Division of Cancer Biology and Inflammatory Disorder, Indian Institute of Chemical Biology, Council of Scientific and Industrial Research (CSIR), 4, Raja S. C Mullick Road, Kolkata 700032, India. Tel.: +91 33 2499 5889; fax: +91 33 2473 0284/5197.
E-mail addresses: tapashi.mandal@gmail.com (T. Mandal), arijitbhoumik@gmail.com (A. Bhowmik), iam_anirban@hotmail.com (A. Chatterjee), uttarac1@gmail.com (U. Chatterjee), sandipchat@gmail.com (S. Chatterjee), mrinal.res@gmail.com (M.K. Ghosh).

http://dx.doi.org/10.1016/j.cellsig.2014.04.003
0898-6568/© 2014 The Authors. Published by Elsevier Inc. This is an open access article under the CC BY-NC-ND license (http://creativecommons.org/licenses/by-nc-nd/3.0/).

and translocation of β-catenin into the nucleus thereby increasing its transcriptional activity [10].

In addition to several substrates already existing for CK2, novel interacting partners are now emerging. It has been recently reported that CK2 activates the Jak–Stat signaling pathway by associating with Jak1 and Jak2 but not Stat3 in myelo-proliferative disorders [11]. Stats are latent transcription factors that mediate cytokine- and growth factor-directed transcription. Stat3 is persistently activated in many human cancers, including glioma, leukemia, myelomas, breast, prostate, pancreatic, lung and ovarian cancers. In tumors, active Stat3 is required for either transformation, enhancing proliferation or blocking apoptosis [12]. The role of Stat3 in GBM pathogenesis is well documented [13–15]. Though Stat3 transcriptional activity is reflected by phosphorylation at both its tyrosine and serine residues, pStat3^{Tyr705} has been implicated in most cases of disease progression [16,17]. Elevated levels of serine phosphorylated Stat3 in GBM have been reported in a single study [18] but the mechanism of activation is poorly understood.

In this study, we focus on the regulation of Stat3 Ser-727 phosphorylation by CK2 in glioma. This regulation was found to be negative and led to increased Stat3 transcriptional activity. Here, PP2A was found to maintain the decreased phosphorylation levels of Stat3 Ser-727 which is controlled by CK2. Reduced Ser-727 phosphorylation of Stat3 with concomitant increase in Tyr-705 phosphorylation leads to enhanced rate of proliferation and invasive property of glioma cells thereby establishing Ser-727 residue of Stat3 to be antagonistic to tumor formation. CK2, thus, crosstalks with the Stat3 signaling pathway through PP2A leading to the progression of more aggressive forms of glioma.

2. Materials and methods

2.1. Cell culture, transfection and drug treatments

The human cell lines HEK293 (embryonic kidney), U87MG, DBTRG-05MG (glioma) and rat cell line C6 (glioma) used in the study were obtained from ATCC (Manassas, VA, USA) and NCCS (Pune, India) respectively. Cells were cultured in DMEM supplemented with 10% heat-inactivated FBS, 2000 units/l penicillin and 2 mg/l streptomycin (Invitrogen, Life Technologies, Grand Island, NY, USA). All cells were maintained at 37 °C in a humid incubator with 5% CO_2. Transfections of different DNA constructs were performed using either Attractene (Qiagen, Gaithersburg, MD, USA) according to manufacturer's instructions or calcium phosphate protocol as described previously [19]. The following drugs/inhibitors, dissolved in DMSO, were used in this study: TBCA (10 μM), LY294002 (20 μM), U0126 (15 μM), and calyculin A (100 nM) (Calbiochem, Darmstadt, Germany), D-sorbitol (0.5 M) and okadaic acid (1 μM) (Sigma Aldrich, Seelze, Germany). Incubation times are indicated in the figure legends. Stable C6 cells were selected using either neomycin (2 mg/ml) or hygromycin (500 μg/ml) depending on the plasmid used.

2.2. Expression plasmids

pGZ21dx-GFP-CK2α, pCDNA3.1 H(+)-Stat3 WT and pCDNA3.1-Stat3-(S727A) were previously described [19,20]. pGZ21dx-GFP-PP2A-Cα plasmid was cloned from HEK293 cells using the primers PP2Acα-F: 5′-AATGAATTCATGGACGAGAAGGTGTTC-3′ and PP2Acα-R: 5′-AATG TCGACCAGGAAGTAGTCTGGGGT-3′. pRS2-(CK2alpha′,CK2beta) and pRS3-(CK2alpha, CK2beta) constructs were obtained from Addgene (Cambridge, MA, USA). All constructs were verified by sequencing.

2.3. Cell lysis, immunoprecipitation and immunoblot analysis

Whole-cell lysates (WCLs) were prepared by lysing the cells in ice-cold buffer as described earlier [21]. SDS-PAGE and Western blot analyses were performed using standard procedures. For coimmunoprecipitation experiments, 1 mg of total protein from lysates was subjected to immunoprecipitation as described previously [22]. Antibodies for pStat3^{Y705}, pStat3^{S727}, Stat3, CK2α, SOCS3 and Bcl-xl were purchased from Cell Signaling Technology (Danvers, MA, USA). Antibodies for MMP9, MMP2, VEGF, Actin and Lamin B were from Santa Cruz Biotechnology (Dallas, Texas, USA). Blots were evaluated by using Enhanced Chemi-luminescence (ECL) reagent according to the manufacturer's protocol (GE Healthcare, Pittsburgh, USA).

2.4. Quantitative real time PCR (qRT-PCR)

Total RNA was extracted using TRIzol reagent (Invitrogen, NY, USA) according to the manufacturer's instructions. For each sample, 2 μg of RNA was converted to cDNA using RevertAid First Strand cDNA Synthesis Kit (Thermo Scientific, Glen Burnie, Maryland, USA) and was subsequently used for qRT-PCR analysis using Power SYBR Green Master Mix on 7500 Fast real time PCR system (Applied Biosystems, Foster City, CA, USA). 18S rRNA (for human glioma cells) and RPL19 (for C6 glioma cells) served as internal controls (normalization) and calibrator controls were chosen appropriately.

Listed below are the primers (human and rat) for the qRT-PCR analysis:

bcl-xl: F-5′-ACCCCAGGGACAGCATATCA-3′,
R-5′-TGCGATCCGACTCACCAATA-3′

SOCS3: F-5′-GGCCACTCTTCAGCATCTC-3′,
R-5′-ATCGTACTGGTCCAGGAACTC-3′

Cyclin D1: F-5′-CCGTCCATGCGGAAGATC-3′,
R-5′-GAAGACCTCCTCCTCGCACT-3′

MCL1: F-5′-AAAGAGGCTGGGATGGGTTT-3′,
R-5′-CAAAAGCCAGCAGCACATTC-3′

18S: F-5′-GCTTAATTTGACTCAACACGG-3′,
R-5′-AGCTATCAATCTGTCAATCCTGTC-3′

BCL2: F-5′-CCGGGAGAACAGGGTATGATAA-3′,
R-5′-CCCACTCGTAGCCCCTCTG-3′

Myc: F-5′-TGTATGTGGAACGGCTTCTC-3′,
R-5′-CCTGGTAGGGGTCCAGCTTC-3′

RPL19: F-5′-ATCGCCAATGCCAACTCT-3′,
R-5′-GAGAATCCGCTTGTTTTTGAA-3′.

2.5. Luciferase reporter assay

c-jun promoter region (−1780 to +731) containing Stat3 binding site (GAS sequence — TTCCCGGAA) was amplified from genomic DNA using sense oligonucleotide: 5′-GAGAATTCCAAGTTCAGAAGCAG-3′ and antisense oligonucleotide: 5′-GAGCTACCCGGCTTTGAAAAGT-3′ containing XhoI and HindIII restriction sites respectively. The resulting fragment was inserted into pGL3-basic plasmid to generate pGL3–c-jun construct. HEK293 or C6 cells were transiently transfected with the pGL3–c-jun construct along with *Renilla* luciferase vector (pRL-TK) and respective gene constructs as per experimental interest. 36 h post-transfection, cells were treated with respective inhibitors or activators for the time periods indicated in the figure legend. Cells were harvested using Dual Luciferase Reporter Assay System (Promega, Madison, USA) following the manufacturer's protocol and measured in VICTOR X Multilabel Plate Reader (PerkinElmer, Waltham, MA, USA). Quantification was based on three independent experiments.

2.6. Immunohistochemistry (IHC) and image scoring

Formalin Fixed Paraffin Embedded (FFPE) post-surgical human glioma tissue samples (n = 23) were collected from patients diagnosed with glioma following all medical and ethical regulations and with formal approval from the ethical committee of both CSIR-IICB and Park Clinic (source). For immunohistochemical staining, previously described protocol was followed [20]. Primary antibodies for pStat3^{S727} and CK2α were from Abcam (MA, USA), while pStat3^{Y705} antibody (XP-monoclonal) was obtained from Cell Signaling Technology (Danvers, MA, USA). Images were captured using DP71 camera (Olympus, Japan) in BX-61 microscope (Olympus, Japan) and analyzed using Image Pro Plus imaging software (Media Cybernetics, Bethesda, USA). A semi-quantitative scoring method was used and H-score was generated as described previously [20] which were used for further statistical analysis. The human samples contained a collection of grade II, III and IV glioma tumor sections (n = 23) with adjacent normal portions wherever possible.

2.7. Immunofluorescence microscopy

C6 cells were subjected to immunofluorescence studies after the indicated treatment according to previously described protocol [23]. Images were captured using DP71 camera in BX-61 microscope and analyzed using Image Pro Plus imaging software.

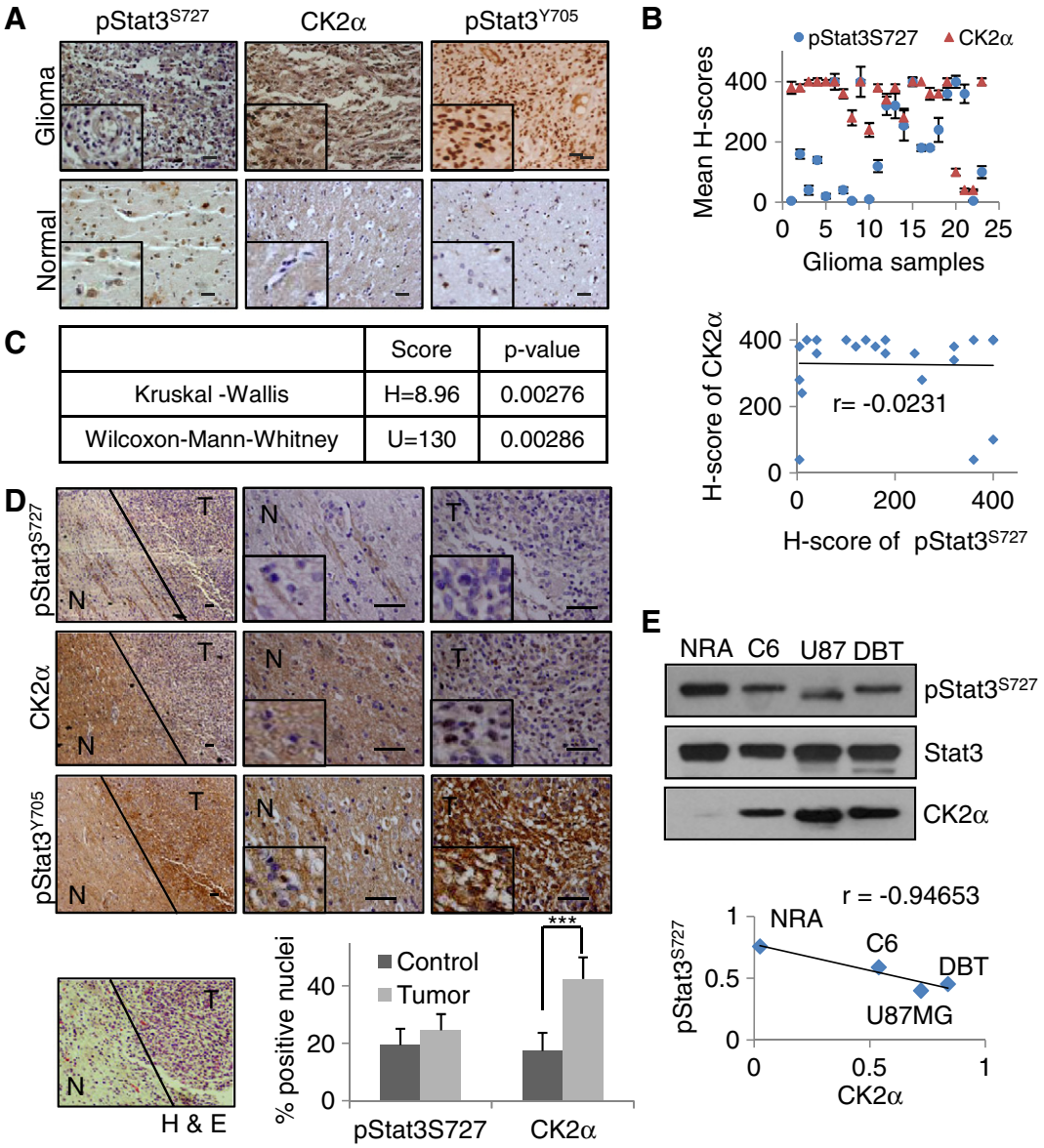

Fig. 1. Phosphorylation of Stat3 at Ser-727 occurs less frequently than CK2 expression in glioma. (A) Representative images of tumor regions taken from 23 human glioma patient samples and adjoining normal brain regions of 6 human glioma patient samples stained with antibodies against pStat3^{S727}, pStat3^{Y705} and CK2α. Images were captured at magnifications of 200×. A section from each image has been magnified in the corresponding insets. (B) Scattered plot representing the mean H-score of the tissue samples (top panel). Graph represents correlation coefficient (r) between the mean H-score of CK2α and pStat3^{S727} (bottom panel). (C) Table depicts the score from Kruskal–Wallis and Wilcoxon–Mann–Whitney statistical analyses. (D) Representative images taken from a section of rat C6 cell line derived intracranial tumor - H & E stained sections and sections immunostained with CK2α, pStat3^{S727} and pStat3^{Y705}. The normal and tumor regions are delineated with a solid line. Images were captured at magnifications of 400× (A section from each image has been magnified in the corresponding insets.) Graph represents percentage of positive nuclei in the normal and tumor regions (***p = 0.0001). (E) Whole cell lysates (WCLs) from normal rat astrocytes (NRA) and glioma cell lines C6 (rat glioma), U87MG and DBT-RG 05MG (human glioma) were immunoblotted to check the levels of pStat3^{S727} and CK2α. Pearson's correlation coefficient (r) between these two proteins is plotted in the graph.

2.8. MTT assay

Cell viability was measured by using MTT [3-(4, 5-dimethylthiazol-2-yl)-2,5-diphenyltetrazolium bromide] which is reduced to purple formazan in the mitochondria of living cells. 10,000 cells/well were seeded in a 96-well plate and allowed to grow for 48 h. Following the removal of culture medium, cells in 96-well plates were incubated with 1 mg/ml MTT for 4 h. The medium was aspirated and the formazan solubilised in 100 μl DMSO. The optical density of each sample at 570 nm was measured in VICTOR X Multilabel Plate Reader (PerkinElmer, Waltham, MA, USA). Quantification was based on three independent experiments.

2.9. Soft-agar colony formation

For soft-agar assays, 2000 cells were suspended in DMEM containing 0.35% agar and layered on top of 1 ml of DMEM solidified with 1.0% agar in each 35 mm dish. After growing at 37 °C for 14 days, colonies were visualized in different microscopic fields and images captured in Olympus IX81 microscope using Image Pro Plus imaging software.

2.10. FACS analysis

Cells were trypsinized and washed in PBS, pelleted, resuspended in ice-cold 70% ethanol for fixation and kept overnight at −20 °C. After washing two times in PBS, cells were resuspended in PI/RNase staining buffer (BD Pharmingen, Franklin Lakes, NJ, USA) and incubated in dark for 15 min at ambient temperature. Cell cycle distribution was examined by flow cytometry using a LSR Fortessa flow cytometer (BD Biosciences, Franklin Lakes, NJ, USA) and analyzed using WinMDI 2.9 software (http://facs.scripps.edu/).

2.11. Matrigel invasion assay

Cell invasion was assayed by using BD Biocoat™ matrigel invasion chambers with 8 μm PET membrane. 50,000 cells were suspended in 0.5 ml of 0.4% serum containing medium and were added to the upper chamber. DMEM containing 10% fetal bovine serum was used as chemoattractant in the lower chamber. The cells were incubated for 16 h in a humidified CO_2 incubator at 37 °C. Cells that traversed the 8 μm membrane pores and spread to the lower surface of the membrane were stained with 5% Giemsa solution and were counted in five

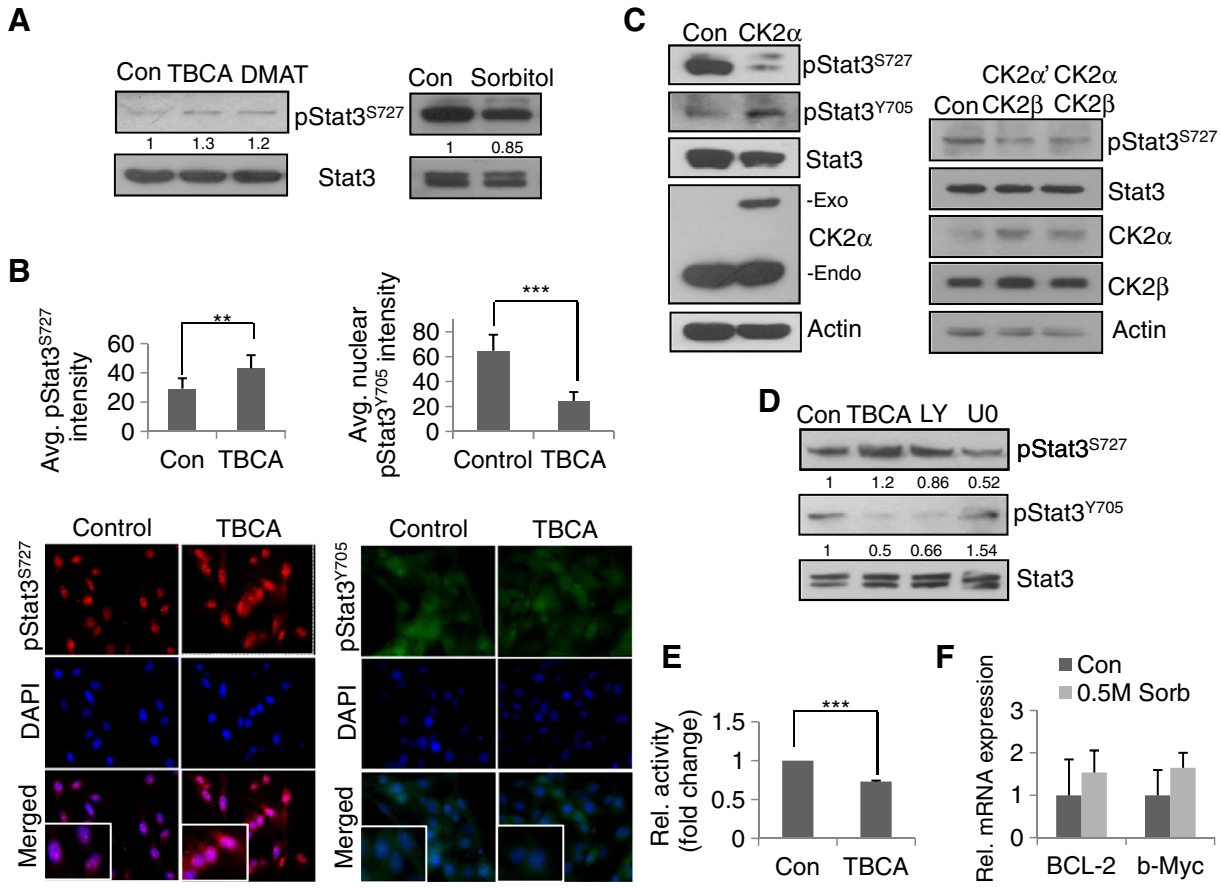

Fig. 2. CK2 negatively regulates phosphorylation of Stat3 at Ser-727 but affects its transcriptional activity positively. (A) C6 cells were treated with inhibitors of CK2 — TBCA or DMAT for 6 h, followed by immunoblotting of WCLs for pStat3^{S727} and Stat3 (left panel). CK2 activity was induced in C6 cells by treatment with 0.5 M sorbitol for 1 h. WCLs were analyzed for pStat3^{S727} and Stat3 (right panel). Comparison of densitometric scan values is with respect to Stat3 intensity. (B) Dimethyl sulfoxide (DMSO) treated control and TBCA treated C6 cells were immunostained with pStat3^{S727} or pStat3^{Y705} (primary) and AlexaFluor594 or AlexaFluor488 (secondary) and observed under a fluorescence microscope. Images were captured along with DAPI stained nuclei at 600× magnification (A section from each merged image has been magnified in the corresponding insets.) Graph represents average pStat3^{S727} staining intensity or pStat3^{Y705} nuclear staining intensity in the control and treated cells (**$p = 0.002$, ***$p = 0.0001$). (C) C6 cells were transfected with WT-CK2α (left panel) and CK2α′-CK2β and CK2α-CK2β (right panel). Lysates were prepared from 36 h post-transfected cells and probed for pStat3^{S727}, pStat3^{Y705}, Stat3 and CK2α (left panel) and pStat3^{S727}, Stat3, CK2α/α′ and CK2β (right panel). (D) C6 cells were treated with inhibitors of CK2, PI3K-Akt and MAPK — TBCA, LY294002 (LY) and U0126 (UO) respectively, for 6 h. WCLs were immunoblotted for pStat3^{S727}, pStat3^{Y705} and Stat3 (Comparison of densitometric scan values is with respect to Stat3 intensity.) (E) C6 cells were transfected with pGL3–c-jun luciferase reporter plasmid. After 42 h of transfection, including the last 6 h with TBCA, WCLs were prepared and luciferase activity was measured in triplicates. Results are presented in terms of fold change and the values represent the mean (±) S.D. from three independent transfections (***$p = 0.001$). (F) C6 cells were treated with 0.5 M sorbitol for 1 h. qRT-PCR analysis of Stat3 target genes was performed using total RNAs extracted from the treated cells.

different fields. Each experiment was carried out in triplicate and error bars represent the mean S.E.

2.12. Orthotopic tumor model

All animal care and experimentation conformed to the CPCSEA guidelines. To generate the tumor model, Sprague–Dawley rats weighing approx. 200 g were intracranially injected with early passage C6 cells (normal and stable cell lines) (1×10^6) once. After 21 days, tissue samples of both tumor and adjacent normal regions of brain were collected and fixed in 10% buffered formalin and embedded in paraffin for further histological and histochemical analysis.

2.13. Syngenic tumor model in flanks

To generate this tumor model, Sprague–Dawley rats were injected with EV, Stat3 WT and Stat3 mutant cells (1×10^6) in the flank region once. Growth of the tumors was observed for a period of 14 days after which the rats were sacrificed and tumors were excised for further analysis.

2.14. Statistical analysis and densitometry

All statistical calculations were done using GraphPad (QuickCalcs, http://www.graphpad.com/quickcalcs/index.cfm) calculator. Scores for U-test and H-test were calculated manually. For the analysis of statistical significance, Student's t-test (unpaired) was used. In all experiments a value of $p < 0.05$ was taken as statistically significant. Quantification of nuclear localized protein and densitometric scanning of immunoblots were done using Image J software (Bethesda, MD, USA).

3. Results

3.1. pStat3^{S727} is less frequent when compared to CK2 expression in glioma

As both CK2 and pStat3^{S727} are oncogenic proteins and has been implicated in GBM, a correlation study between these two proteins was done. Immunohistochemical analysis of tissue samples from 23 human glioma patients (grades II, III and IV) for these two proteins showed perceptible nuclear presence. CK2 is highly overexpressed in glioma whereas the presence of pStat3^{S727} is visibly less when compared to normal sections of the brain tissue (Fig. 1A). In accordance to earlier reports [24], pStat3^{Y705} was found to be overexpressed in the glioma patient samples compared to normal brain samples. The staining intensities of pStat3^{S727} and CK2α proteins were quantified, where a very weak degree of negative correlation was obtained (Pearson's correlation coefficient, $r = -0.0231$) (Fig. 1B). Statistical analysis of the H-scores by Kruskal–Wallis and Wilcoxon–Mann–Whitney tests confirmed that the differences in staining intensities of the two proteins were indeed statistically significant (Fig. 1C).

Next, we tested the existence of correlation between CK2 and pStat3^{S727} in rat glioma, which was proved earlier in human glioma tissues. To examine this, a C6 glioma cell line derived orthotopic tumor model in Sprague–Dawley rats was used. This model has been described extensively in a previous report [22]. Sections from the orthotopic tumors were prepared such that they contained adjacent normal and

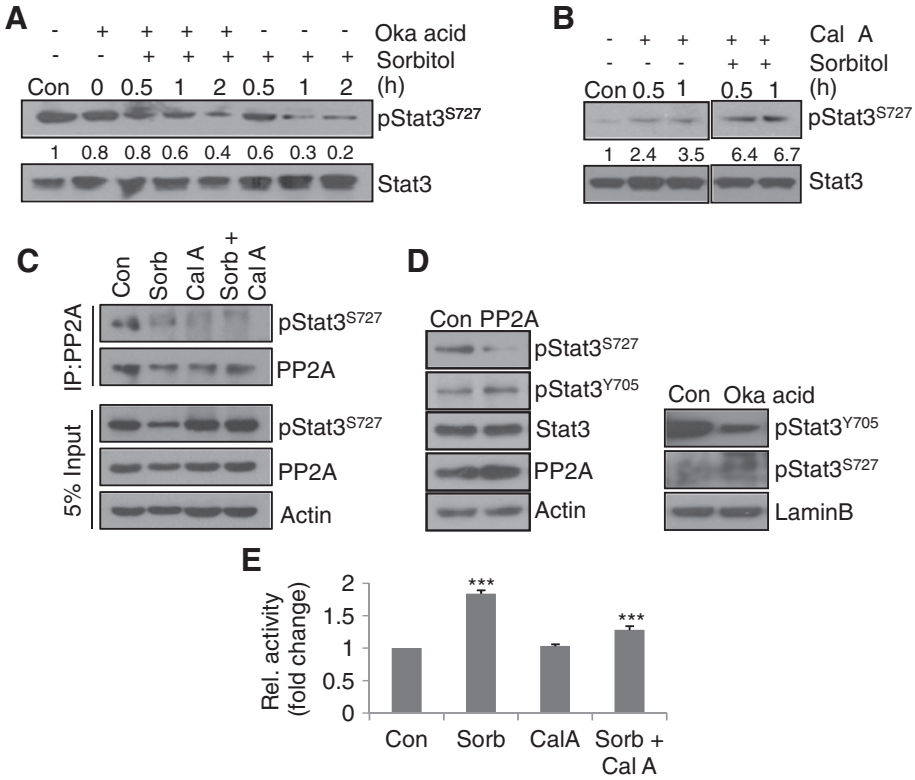

Fig. 3. Dephosphorylation at Stat3 Ser-727 by PP2A causes its negative regulation by CK2. (A) & (B) C6 cells were treated with PP2A inhibitors okadaic acid (4 h) or calyculin A (0.5 and 1 h) in addition to 0.5 M sorbitol for the indicated time periods. WCLs were prepared and immunoblotted for pStat3^{S727} and Stat3. Comparison of densitometric scan values is with respect to Stat3 intensity. (C) C6 cells were treated with 0.5 M sorbitol for 1 h and calyculin A for 0.5 h. WCLs were immunoprecipitated with PP2A and immunoblotted with pStat3^{S727}, PP2A and actin. (D) HEK293 cells were transfected with PP2A-Cα. WCLs were prepared 36 h post transfection and immunoblotted for pStat3^{S727}, pStat3^{Y705}, Stat3 and PP2A (left panel). Nuclear extracts were prepared from C6 cells treated with okadaic acid for 4 h followed by immunoblotting with pStat3^{S727}, pStat3^{Y705} and Lamin B (right panel). (E) HEK293 cells were transfected with pGL3–c-jun luciferase reporter plasmid. After 36 h of transfection, cells were treated with 0.5 M sorbitol for 1 h and/or calyculin A for 0.5 h. Lysates were prepared and luciferase activity was measured in triplicates. Results are presented in terms of fold change and the values represent the mean (±) S.D. from three independent experiments (***$p = 0.0001$ and 0.0011 respectively).

tumor regions, delineated by analysis of gross morphological features by hematoxylin and eosin (H & E) staining. Upon examination of the expression of CK2α and pStat3^{S727} in these tissue sections and quantification of number of positive staining nuclei, it was found that CK2α levels were upregulated in tumors when compared to normal tissue but the change in pStat3^{S727} levels was not quite significant ($p = 0.054$) (Fig. 1D). It was interesting to note that overall cellular CK2α staining intensity remained similar in both normal and tumor regions but its presence was prominent in the nucleus of the tumor cells reflecting its nuclear role in glioma. pStat3^{Y705} levels were found to be increased in tumor regions of rat model as well. When the status of CK2α expression and pStat3^{S727} was checked in normal rat astrocytes and glioma cell lines (C6 rat glioma; U87MG and DBT-RG05MG human glioma), a high degree of negative correlation ($r = -0.94653$) was established (Fig. 1E). Thus, CK2 and pStat3^{S727} both play an important role in glioma and there may exist a mechanism by which these two crucial factors act for glioma progression.

3.2. Phosphorylation of Stat3 at Ser-727 is negatively regulated by CK2

As CK2 and pStat3^{S727} show a negative correlation, we tried to study the molecular mechanism for this phenomenon. To examine this, C6 glioma cells were treated with known inhibitors TBCA and DMAT for CK2. Inhibition of CK2 activity resulted in increased pStat3^{S727} level (Fig. 2A, left panel). On the contrary, enhancing the activity of CK2 by treatment with 0.5 M sorbitol decreased pStat3^{S727} level (Fig. 2A, right panel). Again, immunocytochemical analysis of C6 cells upon CK2 inhibition showed elevated levels of phosphorylated Stat3 at Ser-727 (Fig. 2B, left panel). Conversely, pStat3^{S727} levels were reduced when CK2α, CK2α′ or CK2β was exogenously overexpressed (Fig. 2C). Interestingly, a decrease in pStat3^{S727} levels leads to elevated level of pStat3^{Y705} when CK2 is exogenously overexpressed (Fig. 2C). This reverse effect on Stat3 Ser-727 phosphorylation and Stat3 Tyr-705 phosphorylation was also observed when CK2 was inhibited by TBCA (Fig. 2B, right panel and D). When an inhibitor for MEK pathway, U0126, was used, as expected, pStat3^{S727} phosphorylation was reduced with concomitant increase in pStat3^{Y705} levels (Fig. 2D).

Further, to evaluate whether perturbation in pStat3^{S727} levels resulted in altered transcriptional activity of Stat3, C6 cells were transfected with pGL3–c-jun promoter plasmid, containing Stat3 binding site (GAS sequence — TTCCCGGAA), along with inhibition of CK2 activity. In this context of increased pStat3^{S727} and reduced pStat3^{Y705} levels, Stat3 transcriptional activity was found to reduce significantly (Fig. 2E). When C6 cells were treated with 0.5 M sorbitol, transcription of Stat3 target genes was enhanced upon increased CK2 activity and thereby reduced pStat3^{S727} level (Fig. 2F). CK2, therefore, seems to negatively regulate Stat3 Ser-727 phosphorylation but positively affects its transcriptional activity. Alternatively, it appears that pStat3^{S727} impedes the transcriptional potential of Stat3.

3.3. Negative regulation of Stat3 Ser-727 phosphorylation by CK2 is mediated via PP2A

CK2, being a kinase, has no phosphatase activity. Therefore, its negative regulation of Stat3 Ser-727 phosphorylation warrants the mediation of a third party phosphatase. Overview of literature proposes a serine/threonine protein phosphatase, PP2A, which is regulated by direct interaction with CK2α [25]. PP2A is also known

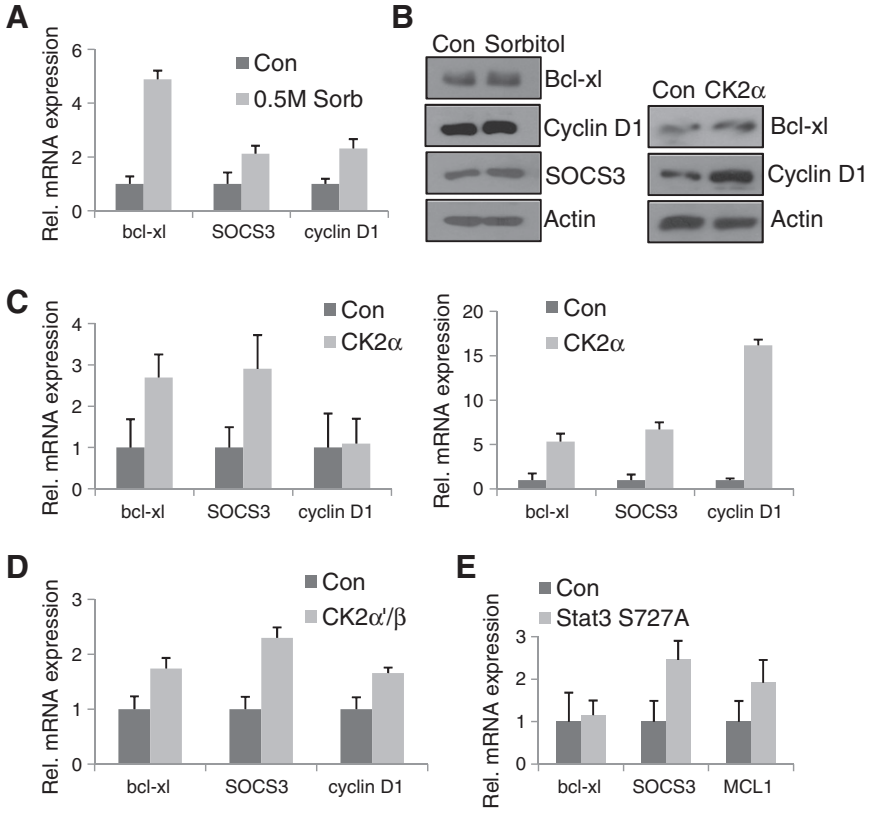

Fig. 4. CK2 activation or overexpression upregulates Stat3 target genes upon reduction of pStat3^{S727}. (A) Glioma cell line DBT-RG05MG was treated with 0.5 M sorbitol for 1 h. qRT-PCR analysis of Stat3 target genes was performed using total RNAs extracted from the treated cells. (B) C6 cells were treated with 0.5 M sorbitol for 1 h or transfected with CK2α. WCLs were prepared and immunoblotted for bcl-xl, Cyclin D1 and SOCS3. (C) HEK293 or U87MG cells were transfected with CK2α followed by total RNA extraction and qRT-PCR analysis of Stat3 target genes. (D) CK2α′/β was transiently transfected in HEK293 cells. 36 h post-transfection, total RNAs were extracted and expressions of Stat3 target genes were analyzed. (E) HEK293 cells were transfected with Stat3 S727A followed by RNA extraction and qRT-PCR analysis of Stat3 target genes. Experiments were repeated three times and values represent the mean (±) SE.

to dephosphorylate Stat3 and influence its activity [26,27]. Consequently, C6 cells were treated with PP2A inhibitors okadaic acid and calyculin A, for the time periods indicated in the figure legend, along with 0.5 M sorbitol which induces CK2 activation. It was noted that sorbitol induced decrease in pStat3^{S727} level was restored significantly when either okadaic acid (Fig. 3A) or calyculin A (Fig. 3B) was used. Although extremely transient, to analyze the possible physical interaction of PP2A and pStat3^{S727}, PP2A was immunoprecipitated and was found to interact with pStat3^{S727} when activated by CK2 in the presence of sorbitol. This interaction was diminished when calyculin A was used because of the reduced activity of PP2A (Fig. 3C). We further found that when PP2A is overexpressed, a decrease in pStat3^{S727} level resulted in increased Stat3 phosphorylation at its Tyr-705 residue (Fig. 3D, left panel). Alternatively, when PP2A activity was inhibited in C6 cells by okadaic acid treatment and nuclear localization of pStat3^{Y705} and pStat3^{S727} was observed, it was found that level of pStat3^{Y705} decreased in the nucleus when compared to the control, whereas there was an increase in pStat3^{S727} level in this condition (Fig. 3D, right panel). Thus, reduced pStat3^{S727} level results in its increased functional activity.

Effect of PP2A inhibition was also noticed upon pGL3–c-jun promoter analysis, where sorbitol induced decrease in pStat3^{S727} levels ensued heightened activity of this promoter which was perceptibly reduced on calyculin A treatment. Further, combined treatment with sorbitol and calyculin A was able to restore the promoter activity partially (Fig. 3E). Accordingly, it may be suggested that activation of CK2 increases the phosphatase activity of PP2A which in turn results in dephosphorylation of Stat3 at Ser-727 thereby augmenting its transcriptional activity.

3.4. Effect of CK2 on the expression of Stat3 target genes

Stat3 is an established oncogenic transcription factor with several targets that include anti-apoptotic proteins like BCL2 family proteins including bcl-xl, MCL-1 and BCL-2, the proliferation-associated proteins Cyclin D1 and c-Myc, pro-angiogenic factor VEGF, its feedback regulator SOCS [28] and several others [12,29,30]. To analyze the effect of CK2 mediated downregulation of pStat3^{S727} on its downstream effectors, qRT-PCR was done in various cell lines including DBT-RG05MG, U87MG and HEK293. It was found that concomitant with our results obtained from luciferase reporter assays, decreased pStat3^{S727} levels upon sorbitol treatment or CK2α, CK2α′ and CK2β overexpression favored its transcriptional activity which was translated into increased expression of SOCS3, bcl-xl and Cyclin D1 genes in the human cell lines (Fig. 4A, C and D). Increased levels of Stat3 target proteins SOCS3, bcl-xl and Cyclin D1 were also observed upon overexpression or activation of CK2 (Fig. 4B).

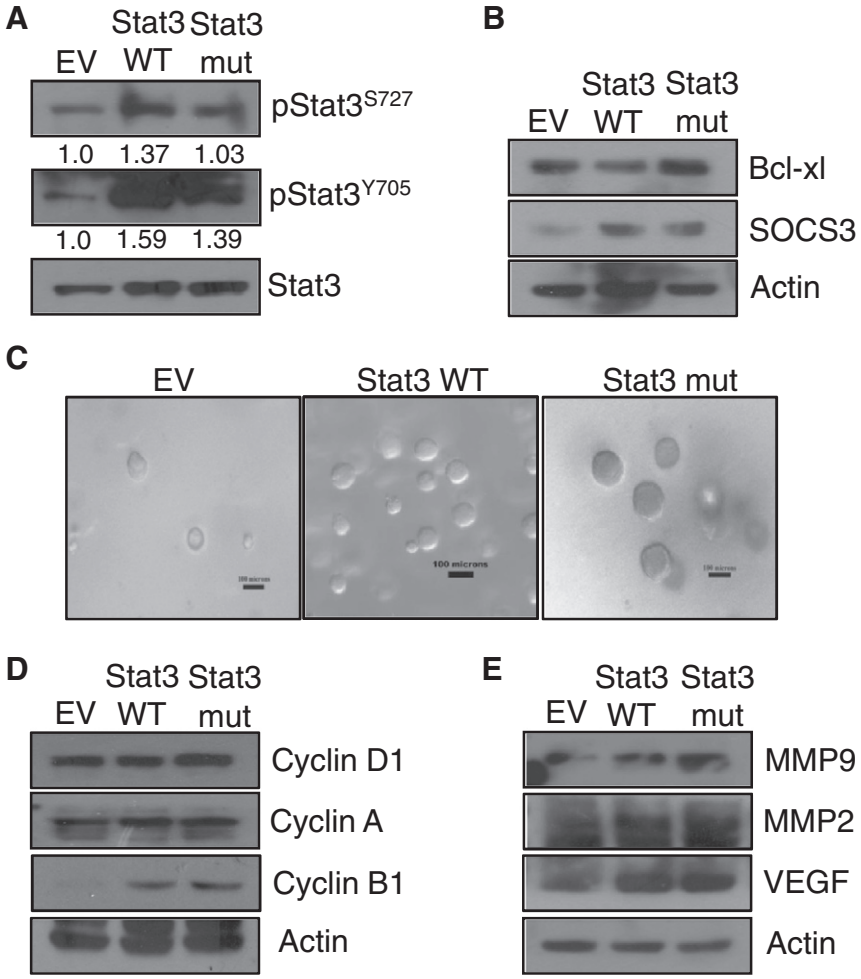

Fig. 5. Reduction of Stat3 Ser-727 phosphorylation promotes oncogenic role of Stat3. (A) Rat C6 glioma cells were stably transfected and selected for Stat3 WT, Stat3 S727A mutant and empty vector (EV) control. Phosphorylation status of Stat3 at Ser-727 and Tyr-705 was checked in the WCLs of these stable cells. (B) Levels of Stat3 downstream targets bcl-xl and SOCS3 were analyzed by immunoblotting of WCLs from EV, Stat3 WT and mutant cells. (C) C6 cell lines stably expressing the EV, Stat3 WT or mutant were plated in soft-agar at a density of 2000 cells per 35 mm dish. After incubation for 14 days, colonies were visualized under microscope and images captured at 200× magnification. (D & E) WCLs of EV, Stat3 WT or mutant cells were immunoblotted for Cyclin D1, Cyclin A and Cyclin B1 (cell cycle proteins) or MMP9, MMP2 and VEGF (angiogenic proteins).

To mimic the decreased phosphorylated state of pStat3^{S727} due to overexpression or activation of CK2, HEK293 cells were transiently transfected with the plasmid containing Stat3 serine mutant, Stat3 S727A. The effect was similar and the mutant plasmid was also able to increase the expression of bcl-xl, SOCS3 and MCL1 genes (Fig. 4E). Thus, it is inferred that Stat3 Ser-727 phosphorylation acts antagonistically to its Tyr-705 phosphorylation in this context thereby affecting its transcriptional activity negatively. Collectively, removal of the Ser-727 phosphorylation mediated by CK2–PP2A augments the expression of several pro-survival and proliferative proteins which may ultimately lead to cancer progression.

3.5. Reduced phosphorylation at Ser-727 residue enhances oncogenic potential of Stat3

As evident from our findings, decreased Stat3 Ser-727 phosphorylation resulted in increased transcription of its downstream targets. This effect was observed either by CK2 overexpression or ectopic expression of Stat3 S727A mutant; which may be ultimately imperative in promoting tumor progression. To confirm this possibility, constitutively expressing stable C6 cell lines harboring either the Stat3 WT or Stat3 S727A mutation was established. Expectedly, pStat3^{Y705} levels were high in both cell lines when compared to the EV control (Fig. 5A). Phosphorylation at Stat3 Ser-727 residue was also high in the Stat3 WT cells when compared to the EV or mutant cells. When the effect of these phosphorylation changes was analyzed in downstream proteins, it was observed that though the expression of SOCS3 increased in both cell types when compared to EV control, level of bcl-xl, a well known survival protein, was highly increased in the Stat3 mutant cells which may be due to the negative regulation of Stat3 DNA binding activity by its Ser-727 phosphorylation (Fig. 5B). The rate of cell proliferation was also found to be more in the mutant cells compared to the WT and EV control cells as assessed by MTT proliferation assay (Fig. S1). To determine the anchorage independent growth potential of the Stat3 mutant cell line, soft-agar colony formation assay was performed. Again, the mutant cells produced relatively larger colonies than both the WT and EV control cells (Fig. 5C). Increased proliferative capacity of the Stat3 S727A mutant cells was further confirmed by analysis of the cell cycle proteins, Cyclin D1, Cyclin A and Cyclin B1 (Fig. 5D). Cell cycle analysis by FACS also corroborated this conclusion as more number of cells was in the S and G2/M phases in the mutant cells compared to either the WT or EV control cells (Fig. S2).

To be metastatic and tumorigenic, cancer cells need to invade through basement matrix of tissues and infiltrate surrounding regions.

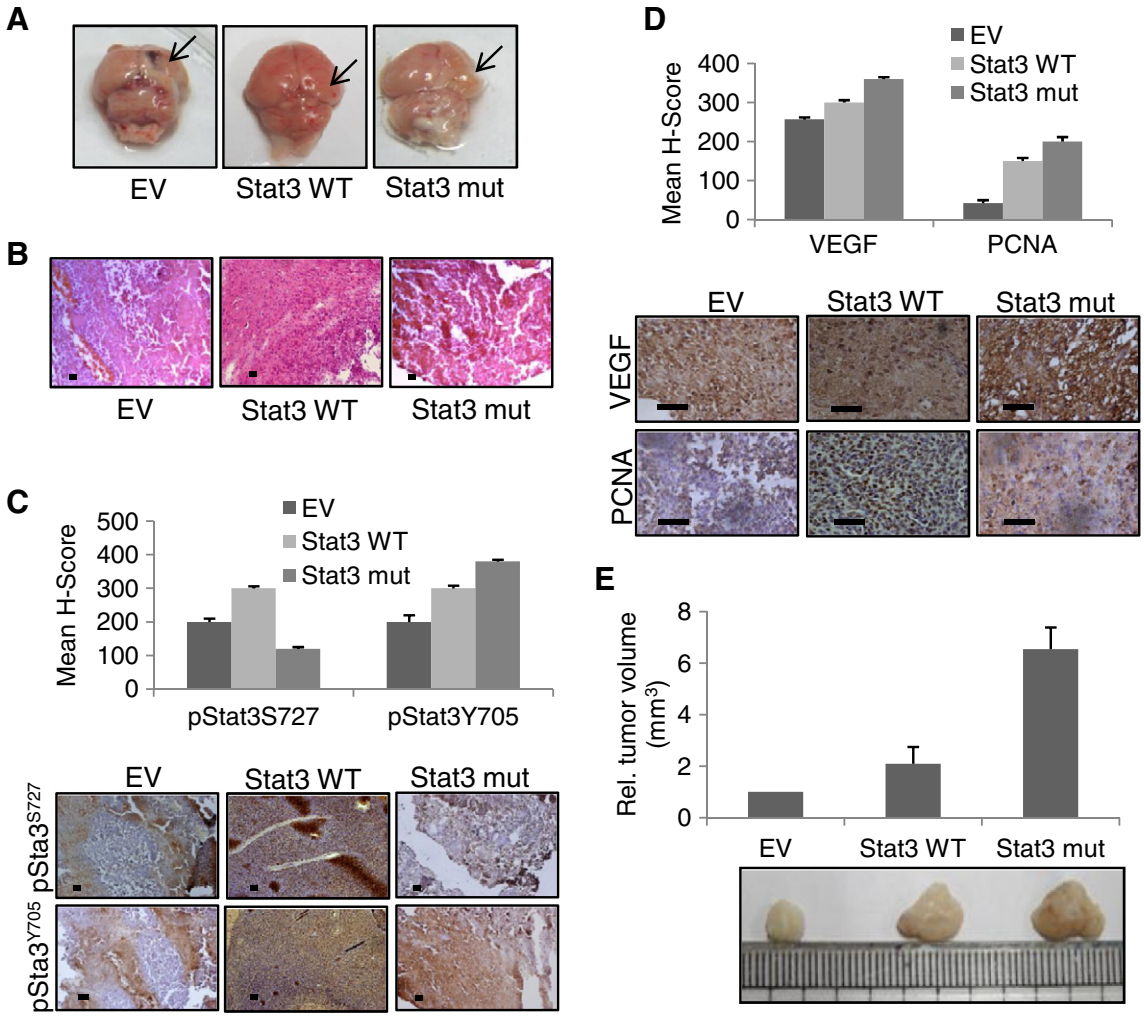

Fig. 6. Reduced phosphorylation of Stat3 at its Ser-727 residue forms more aggressive tumors. (A) Orthotopic tumor model in rat brain obtained by intracranial injection of EV, Stat3 WT and mutant stable cells. (B) Representative image of the H & E stained sections of the orthotopic tumors. (C) Images taken from a section of the intracranial tumors immunostained with either pStat3^{S727} or pStat3^{Y705} antibodies. Images were captured at magnifications of 100×. Graph represents a comparative analysis of H-score of the above proteins in EV, Stat3 WT and mutant stable cell derived tumors. (D) Representative images of the tumor sections immunostained for VEGF or PCNA. Images were captured at magnifications of 400×. Graph represents a comparative analysis of H-score of the above proteins in EV, Stat3 WT and mutant stable cell derived tumors. (E) Tumors obtained from the flank region of the rats were analyzed for tumor volume (top panel) and tumor size (bottom panel).

MMP2 and 9, proteins involved in breakdown of extracellular matrix and VEGF, which increases vascular permeability and angiogenesis showed increased expression in the mutant cells compared to both the WT and EV (Fig. 5E). Interestingly, these proteins are also Stat3 transcriptional targets [31–34]. Matrigel invasion assay conducted to assess the invasive potential of these cells showed more number of cells migrating to the lower compartment of the Boyden chamber in case of the mutant cells compared to the EV control (Fig. S3). Hence, increased transcriptional activity of the Stat3 S727A mutant cells resulted in increased proliferative, metastatic and angiogenic potentials of these cells, which are hallmarks of cancer [35], marking them for cancer progression.

3.6. Reduced pStat3^{S727} levels lead to the development of more aggressive tumors in vivo

To confirm that the Stat3 S727A mutant cells indeed have enhanced tumorigenic potential, the EV, Stat3 WT and Stat3 mutant cells were injected into respective rat brains to create an orthotopic tumor model. Tumors were obtained after approx. 3 weeks (Fig. 6A) and their morphological features were ascertained by H & E staining (Figs. 6B and S4). Immunohistochemical analysis of the tumor sections confirmed that pStat3^{S727} levels were less and pStat3^{Y705} levels were more in Stat3 mutant cells generated tumors when compared to the WT or EV generated ones (Fig. 6C). Increased expression of PCNA and VEGF, markers for cell proliferation and angiogenesis, was also found in the Stat3 mutant generated tumor when compared to WT or EV generated one (Fig. 6D). To determine if the Stat3 mutant cells could form more aggressive tumors, the WT, mutant and EV cells were injected into flanks of SD rats and tumor development was monitored progressively up to 14 days (Fig. S5). Comparison of size and volume of tumors (Fig. 6E) from the three sets of rats confirmed our hypothesis that the Stat3 S727A mutant cells had increased tumorigenic potential and could form more aggressive tumors when compared to either the WT or EV cells.

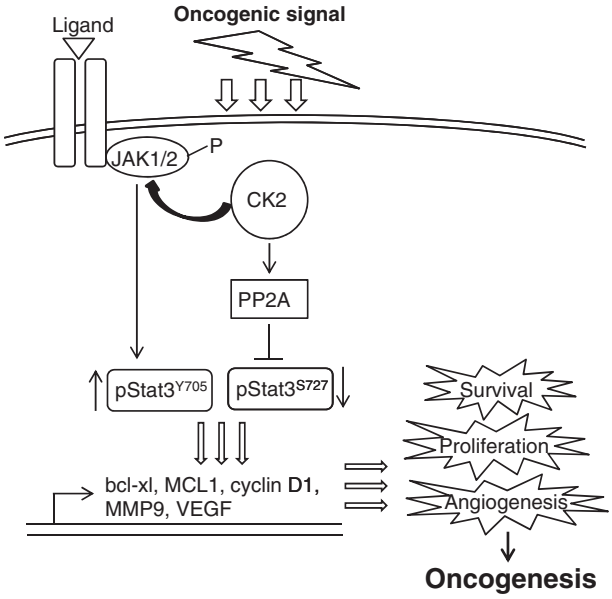

Fig. 7. This model depicts the regulation of Stat3 Ser-727 phosphorylation by CK2 and the ensuing effect on cell survival, proliferation and angiogenesis. Upon stimulation by an oncogenic signal, CK2 gets activated which in turn can phosphorylate Jak2 and induce Stat3 Tyr-705 phosphorylation. Alternatively, CK2 can also induce the activity of a protein phosphatase, PP2A, which then dephosphorylates Stat3 at Ser-727 residue. Reduction of Stat3 Ser-727 phosphorylation by CK2 leads to enhanced Stat3 activity and heightened expression of its target genes. Increased cell survival, proliferation and angiogenesis follow leading to more aggressive tumor progression.

4. Discussion

Oncogenic role of Stat3 is a much established fact and warrants no further discussion [12,29,36]. Activation of this protein is mainly by phosphorylation at its Tyr-705 residue whereby it dimerizes, enters the nucleus and mediates its role as a transcription factor [29]. Apart from this, several reports have entailed phosphorylation of Stat3 at Ser-727 residue to be another important event for the regulation of its transcriptional activity. Stat3 Ser-727 phosphorylation has been reported to be effected by various kinases like Erk, H7 sensitive kinase, protein kinase Cδ, nemo-like kinase, cyclin-dependent kinase 5, mammalian target of rapamycin kinase, death-associated protein kinase 3 and mitogen- and stress activated kinase 1 depending on the cytokine stimulation and the type of cell used for the experiment [37–41]. On evaluating the role of pStat3^{S727}, it was found that it could either positively affect the Stat3-mediated gene activation [42,43] or repress the activity of Stat3 [19,37,41]. Another report also suggests that there may be no effect on Stat3 DNA binding activity as a result of Stat3 Ser-727 phosphorylation [44]. This contradictory role of Stat3 Ser-727 phosphorylation may be due to the different stimulus used or the difference in cellular environment which leads to altered post-translational modifications of proteins thus affecting their function. In certain tumors, where Stat3 was implicated for oncogenesis, activation of Stat3 was found to be the result of phosphorylation at both Tyr-705 and Ser-727 residues [36,45–47]. Although no report till date details the role of pStat3^{S727} in glioma progression, elevated levels of this phoshoprotein have been reported in GBM patient samples but not in GBM cell lines [18]. Contrary to this finding of Brantley et al., we found that pStat3^{S727} was negligibly elevated in glioma when compared to normal tissue and was either cytoplasmic or poorly localized in the nucleus of tumor samples. The level of pStat3^{S727} was also reduced in glioma cell lines when compared to normal rat astrocytes suggesting a deleterious effect of this form of Stat3 on glioma progression. The regulation of this post-translational modification of Stat3, therefore, is vital in glioma pathogenesis.

Novel regulatory mechanisms of Stat3 Ser-727 phosphorylation may lead to better understanding of the nature of tumor progression. In our study, we checked the effect of a serine/threonine kinase CK2 in pStat3^{S727} regulation; CK2 is known to activate the Jak–Stat signaling pathway via interaction with Jak2 [11] which mediates phosphorylation of Stat3 at Tyr-705 residue. Supporting the report by Dixit et al. [7], we found heightened CK2α expression in glioma, which was prominently nuclear in tumor cells, substantiating its pro-oncogenic role and also exhibiting a converse relation to pStat3^{S727} levels. As expected, upon overexpression, CK2α could induce Stat3 transcriptional activity as a result of reduced pStat3^{S727} level with concomitant increase in pStat3^{Y705} level. The negative relationship between pStat3^{S727} and pStat3^{Y705} has been discussed in previous reports where enhancement in pStat3^{S727} levels was associated with decreased pStat3^{705} levels and reduced transcriptional activity [48,49]. Wakahara et al. have proposed a mechanism for this negative regulation which works largely through a protein tyrosine phosphatase, TC45 [41]. That the reduced Ser-727 phosphorylation level of Stat3 was responsible for its enhanced transcriptional activity in our findings provide an insight as to why the pStat3^{S727} level is not enhanced in glioma when compared to normal tissues.

PP2A forms stable complexes with various protein molecules, thereby establishing itself to be a major regulator in cellular signaling by reversible protein phosphorylation. Though PP2A has been suggested to be a tumor suppressor [50], caution must be exercised before referring to the different PP2A complexes in generic terms. Reports exist where PP2A tumor suppressive activity has been inhibited for the promotion of cellular transformation [51–53]. Indeed, in our study, we suggest PP2A to have an indirect tumor promoting function by dephosphorylating Stat3 Ser-727 which in turn increases the transcriptional activity of Stat3. Thus, in glioma, CK2 may play its pro-oncogenic role by associating with PP2A, activating it and resulting in altered activity of Stat3.

Corollary to our c-jun promoter analysis studies, increased transcriptional activity of Stat3 upon reduced phosphorylation at its Ser-727 residue was reflected in the increased expression of its target genes like bcl-xl, SOCS3, MCL1 and Cyclin D1. As these genes are involved in cell survival (BCL-2 family genes) and cell cycle (Cyclin D1), a stable cell line overexpressing the Stat3 S727A mutant had a greater survival and proliferative capacity. These cells were also more invasive and expressed increased amount of the angiogenic protein VEGF, distinguishing them as precursors to cancer progression. Indeed, these cells could also form larger tumors *in vivo*. Thus, Stat3 activation by reduced Ser-727 phosphorylation confers multiple advantages on the glioma cells that are essential for successful malignancy (See Fig. 7). Targeting Stat3 activity has been the method of choice for therapies against cancer [54–56] and our study provides a novel axis for exploration in this direction.

5. Conclusions

In our study we establish that i) Stat3 activity is regulated by CK2 at its Ser-727 residue, ii) PP2A is activated upon CK2 activation and acts as the dephosphorylating agent for $pStat3^{S727}$, iii) Stat3 Ser-727 mutant cell line could enhance glioma cell survival, proliferation and invasion, and iv) *In vivo* rat model grew more aggressive tumors due to reduced level of $pStat3^{S727}$ with enhanced $pStat3^{Y705}$ level. Thus our study elucidates a novel axis for Stat3 activation which may be targeted for effective glioma therapy.

Acknowledgments

We acknowledge Addgene (Cambridge, MA, USA) for providing the plasmids: pRS2-(CK2alpha′,CK2beta) (27,093) and pRS3-(CK2alpha, CK2beta) (27,092). This work was financially supported by CSIR (EMPOWER-OLP-2, MEDCHEM-BSC0108 and miND-BSC0115).

Appendix A. Supplementary data

Supplementary data to this article can be found online at http://dx.doi.org/10.1016/j.cellsig.2014.04.003.

References

[1] H. Ohgaki, P. Kleihues, Cancer Sci. 100 (2009) 2235–2241.
[2] R.D. Rao, C.D. James, Semin. Oncol. 31 (2004) 595–604.
[3] H. Ji, Z. Lu, Clin. Cancer Res. Off. J. Am. Assoc. Cancer Res. 19 (2013) 6335–6337.
[4] B. Boldyreff, U. Mietens, O.G. Issinger, FEBS Lett. 379 (1996) 153–156.
[5] M. Montenarh, Cell Tissue Res. 342 (2010) 139–146.
[6] G. Cozza, L.A. Pinna, S. Moro, Curr. Med. Chem. 20 (2013) 671–693.
[7] D. Dixit, V. Sharma, S. Ghosh, V.S. Mehta, E. Sen, Cell Death Dis. 3 (2012) e271.
[8] R. Prudent, V. Moucadel, C.-H. Nguyen, C. Barette, F. Schmidt, J.-C. Florent, et al., Cancer Res. 70 (2010) 9865–9874.
[9] P. Robe, Int. J. Oncol. (2012) 776–782.
[10] H. Ji, J. Wang, H. Nika, D. Hawke, S. Keezer, Q. Ge, et al., Mol. Cell 36 (2009) 547–559.
[11] Y. Zheng, H. Qin, S.J. Frank, L. Deng, D.W. Litchfield, A. Tefferi, et al., Blood 118 (2011) 156–166.
[12] J.F. Bromberg, M.H. Wrzeszczynska, G. Devgan, Y. Zhao, R.G. Pestell, C. Albanese, et al., Cell 98 (1999) 295–303.
[13] M. Priester, E. Copanaki, V. Vafaizadeh, S. Hensel, C. Bernreuther, M. Glatzel, et al., Neurosci. Oncol. 15 (2013) 840–852.
[14] S. Kohsaka, L. Wang, K. Yachi, R. Mahabir, T. Narita, T. Itoh, et al., Mol. Cancer Ther. 11 (2012) 1289–1299.
[15] S.O. Rahaman, P.C. Harbor, O. Chernova, G.H. Barnet, M.A. Vogelbaum, S.J. Haque, Oncogene 21 (2002) 8404–8413.
[16] C.-J. Li, Y.-C. Li, D.-R. Zhang, J.-H. Pan, J. Cancer Res. Ther. 9 (2013) S67–S73 (Suppl.).
[17] X. Wei, G. Wang, W. Li, X. Hu, Q. Huang, K. Xu, et al., Oncol. Rep. 31 (2014) 335–341.
[18] E.C. Brantley, L.B. Nabors, G.Y. Gillespie, Y.-H. Choi, C.A. Palmer, K. Harrison, et al., Clin. Cancer Res. 14 (2008) 4694–4704.
[19] M.K. Ghosh, P. Sharma, P.C. Harbor, S.O. Rahaman, S.J. Haque, Oncogene 24 (2005) 7290–7300.
[20] A. Chatterjee, U. Chatterjee, M.K. Ghosh, Cell Death Dis. 4 (2013) e543.
[21] K.K.N. Guturi, T. Mandal, A. Chatterjee, M. Sarkar, S. Bhattacharya, U. Chatterjee, et al., J. Biol. Chem. 287 (2012) 18287–18296.
[22] I. Paul, S.F. Ahmed, A. Bhowmik, S. Deb, M.K. Ghosh, Oncogene 32 (2013) 1284–1295.
[23] S.F. Ahmed, S. Deb, I. Paul, A. Chatterjee, T. Mandal, U. Chatterjee, et al., J. Biol. Chem. 287 (2012) 15996–16006.
[24] L.K. Schaefer, Z. Ren, G.N. Fuller, T.S. Schaefer, Oncogene 21 (2002) 2058–2065.
[25] J.K. Hériché, F. Lebrin, T. Rabilloud, D. Leroy, E.M. Chambaz, Y. Goldberg, Science 276 (1997) 952–955.
[26] S. Togi, S. Kamitani, S. Kawakami, O. Ikeda, R. Muromoto, A. Nanbo, et al., Biochem. Biophys. Res. Commun. 379 (2009) 616–620.
[27] A. Woetmann, M. Nielsen, S.T. Christensen, J. Brockdorff, K. Kaltoft, A.M. Engel, et al., Proc. Natl. Acad. Sci. U. S. A. 96 (1999) 10620–10625.
[28] Y. Lu, S. Fukuyama, R. Yoshida, T. Kobayashi, K. Saeki, H. Shiraishi, et al., J. Biol. Chem. 281 (2006) 36683–36690.
[29] J. Bromberg, J. Clin. Invest. 109 (2002) 1139–1142.
[30] D.E. Levy, C. Lee, J. Clin. Invest. 109 (2002) 1143–1148.
[31] J.E. Jung, H.G. Lee, I.H. Cho, D.H. Chung, S.-H. Yoon, Y.M. Yang, et al., FASEB J. 19 (2005) 1296–1298.
[32] G. Niu, K.L. Wright, M. Huang, L. Song, E. Huara, J. Turkson, et al., Oncogene 21 (2002) 2000–2008.
[33] T.N. Dechow, L. Pedranzini, A. Leitch, K. Leslie, W.L. Gerald, I. Linkov, et al., Proc. Natl. Acad. Sci. U. S. A. 101 (2004) 10602–10607.
[34] Y. Song, L. Qian, S. Song, L. Chen, Y. Zhang, G. Yuan, et al., Mol. Immunol. 45 (2008) 137–143.
[35] D. Hanahan, R.A. Weinberg, Cell 144 (2011) 646–674.
[36] T. Bowman, R. Garcia, J. Turkson, R. Jove, Oncogene 19 (2000) 2474–2488.
[37] J. Chung, E. Uchida, T.C. Grammer, J. Blenis, Mol. Cell. Biol. 17 (1997) 6508–6516.
[38] T. Decker, P. Kovarik, Oncogene 19 (2000) 2628–2637.
[39] N. Jain, T. Zhang, W.H. Kee, W. Li, X. Cao, J. Biol. Chem. 274 (1999) 24392–24400.
[40] K. Yokogami, S. Wakisaka, J. Avruch, S.A. Reeves, Curr. Biol. CB. 10 (2000) 47–50.
[41] R. Wakahara, H. Kunimoto, K. Tanino, H. Kojima, A. Inoue, H. Shintaku, et al., Genes Cells. 17 (2012) 132–145.
[42] S. Aznar, P.F. Valeron, S.V. del Rincon, L.F. Perez, R. Perona, J.C. Lacal, Mol. Biol. Cell 12 (2001) 3282–3294.
[43] Z. Wen, Z. Zhong, J.E. Darnell Jr., Cell 82 (1995) 241–250.
[44] Z. Wen, J.E. Darnell Jr., Nucleic Acids Res. 25 (1997) 2062–2067.
[45] D.J. Kim, K.S. Chan, S. Sano, J. Digiovanni, Mol. Carcinog. 46 (2007) 725–731.
[46] I. Hazan-Halevy, D. Harris, Z. Liu, J. Liu, P. Li, X. Chen, et al., Blood 115 (2010) 2852–2863.
[47] H. Lee, A. Herrmann, J.-H. Deng, M. Kujawski, G. Niu, Z. Li, et al., Cancer Cell 15 (2009) 283–293.
[48] C.X. Andersson, V.R. Sopasakis, E. Wallerstedt, U. Smith, J. Biol. Chem. 282 (2007) 9430–9435.
[49] X. Shi, H. Zhang, H. Paddon, G. Lee, X. Cao, S. Pelech, Biochemistry (Mosc) 45 (2006) 5857–5867.
[50] J. Westermarck, W.C. Hahn, Trends Mol. Med. 14 (2008) 152–160.
[51] P. Neviani, R. Santhanam, R. Trotta, M. Notari, B.W. Blaser, S. Liu, et al., Cancer Cell 8 (2005) 355–368.
[52] M.R. Junttila, P. Puustinen, M. Niemelä, R. Ahola, H. Arnold, T. Böttzauw, et al., Cell 130 (2007) 51–62.
[53] M. Mumby, Cell 130 (2007) 21–24.
[54] M. Zhao, B. Jiang, F.-H. Gao, Curr. Med. Chem. 18 (2011) 4012–4018.
[55] F. Madoux, M. Koenig, E. Nelson, S. Chowdhury, M. Cameron, B. Mercer, et al., Probe Rep. NIH Mol. Libr. Program, National Center for Biotechnology Information (US), Bethesda (MD), 2010.
[56] S.R. Walker, M. Xiang, D.A. Frank, Mol. Cell. Endocrinol. 382 (2014) 616–621